

# Slowly Rotating Anisotropic Neutron Stars in General Relativity and Scalar-Tensor Theory

Hector O. Silva<sup>1</sup>, Caio F. B. Macedo<sup>2</sup>, Emanuele Berti<sup>1,3</sup>,  
Luís C. B. Crispino<sup>2</sup>

<sup>1</sup>Department of Physics and Astronomy, The University of Mississippi,  
University, MS 38677, USA

<sup>2</sup>Faculdade de Física, Universidade Federal do Pará, 66075-110, Belém, Pará,  
Brazil

<sup>3</sup>CENTRA, Departamento de Física, Instituto Superior Técnico, Universidade  
de Lisboa, Avenida Rovisco Pais 1, 1049 Lisboa, Portugal

E-mail: hosilva@phy.olemiss.edu, caiomacedo@ufpa.br, crispino@ufpa.br,  
eberti@olemiss.edu

**Abstract.** Some models (such as the Skyrme model, a low-energy effective field theory for QCD) suggest that the high-density matter prevailing in neutron star interiors may be significantly anisotropic. Anisotropy is known to affect the bulk properties of nonrotating neutron stars in General Relativity. In this paper we study the effects of anisotropy on slowly rotating stars in General Relativity. We also consider one of the most popular extensions of Einstein's theory, namely scalar-tensor theories allowing for spontaneous scalarization (a phase transition similar to spontaneous magnetization in ferromagnetic materials). Anisotropy affects the moment of inertia of neutron stars (a quantity that could potentially be measured in binary pulsar systems) in both theories. We find that the effects of scalarization increase (decrease) when the tangential pressure is bigger (smaller) than the radial pressure, and we present a simple criterion to determine the onset of scalarization by linearizing the scalar-field equation. Our calculations suggest that binary pulsar observations may constrain the degree of anisotropy or even, more optimistically, provide evidence for anisotropy in neutron star cores.

PACS numbers: 04.40.Dg, 04.20.-q, 04.50.Kd, 21.65.Mn, 26.60.Kp

## 1. Introduction

Most investigations of the structure of neutron stars (NSs) assume isotropic matter with a perfect-fluid equation of state (EoS) relating the pressure and density in the stellar interior. However, various physical effects can lead to local anisotropies (see [1] for a review). Anisotropy can occur for stars with a solid core [2] or strong magnetic fields [3, 4, 5]. Spaghetti- and lasagna-like structures would induce anisotropic elastic properties that could be important for NS quakes [6]. Nuclear matter may be anisotropic at very high densities [7, 8], where the nuclear interactions must be treated relativistically and phase transitions (e.g. to pion condensates [9] or to a superfluid state [10]) may occur. For example, Nelmes and Piette [11] recently considered NS structure within the Skyrme model, a low energy, effective field theory for Quantum Chromodynamics (QCD), finding significant anisotropic strains for stars with mass  $M \gtrsim 1.5M_{\odot}$  (see also [12, 13]). From a mathematical point of view, two-fluid systems

can be shown to be equivalent to a single anisotropic fluid [14]. Anisotropy affects the bulk observable properties of NSs, such as the mass-radius relation and the surface redshift [15]: it can increase the maximum NS mass for a given EoS [15, 16] and stabilize otherwise unstable stellar configurations [17]. Incidentally, exotic objects such as gravastars [18] and boson stars [19, 20] are also equivalent to anisotropic fluids (i.e., they have anisotropic pressure).

It is known that rotation can induce anisotropy in the pressure due to anisotropic velocity distributions in low-density systems [1], but to the best of our knowledge – with the exception of some work by Bayin [21] – slowly rotating anisotropic stars have never been investigated in General Relativity (GR). The goal of this paper is to fill this gap using two different phenomenological models for anisotropy [15, 16], and to extend the analysis of slowly rotating anisotropic stars to scalar-tensor theories of gravity.

Scalar-tensor theories are among the simplest and best studied extensions of GR [22]. In addition to the metric, in these theories gravity is also mediated by a scalar field. Scalar-tensor theories arise naturally from the dimensional reduction of higher-dimensional proposals to unify gravity with the Standard Model, and they encompass  $f(R)$  theories of gravity as special cases [23, 24]. The simplest variant of scalar-tensor theory, Brans-Dicke theory, is tightly constrained experimentally [25], but certain versions of the theory could in principle differ from GR by experimentally measurable amounts in the strong-field regime, as shown by Damour and Esposito-Farèse [26, 27].

From an astrophysical standpoint, compact objects such as black holes and NSs are the most plausible candidates to test strong-field gravity [28]. Compared to black holes, NSs are a more promising strong-field laboratory to distinguish scalar-tensor gravity from GR, because a large class of scalar-tensor theories admits the *same* black-hole solutions as GR (see [29] and references therein), and the dynamics of black holes can differ from GR only if the black holes are surrounded by exotic forms of matter [30, 31, 32, 33] or if the asymptotic behavior of the scalar field is nontrivial [34, 35].

The study of NS structure in GR is textbook material [36, 37, 38, 39], and there is an extensive literature on stellar configurations in scalar-tensor theories as well (see e.g. [40, 41] and references therein). One of the most intriguing phenomena in this context is “spontaneous scalarization” [27], a phase transition analogous to the familiar spontaneous magnetization in solid state physics [42]: in a certain range of central densities, asymptotically flat solutions with a nonzero scalar field are possible and energetically favored with respect to the corresponding GR solutions.

In the absence of anisotropy, the degree of scalarization depends on a certain (real) theory parameter  $\beta$ , defined in Eq. (2) below. Theory predicts that scalarization cannot occur (in the absence of anisotropy) when  $\beta \gtrsim -4.35$  [43]. Present binary pulsar observations yield a rather tight experimental constraint:  $\beta \gtrsim -4.5$  [44, 45]. One of our main findings is that the effects of scalarization, as well as the critical  $|\beta|$  for spontaneous scalarization to occur, increase (decrease) for configurations in which the tangential pressure is bigger (smaller) than the radial pressure. Therefore binary pulsars can be used to constrain the degree of anisotropy at fixed  $\beta$ , or to constrain  $\beta$  for a given degree of anisotropy. This may open the door to experimental constraints on the Skyrme model via binary pulsar observations. Other notable findings of this study are (i) an investigation of the dependence of the stellar moment of inertia on the degree of anisotropy  $\lambda$  (more precisely,  $\lambda_H$  and  $\lambda_{BL}$ , because we consider two different anisotropy models [15, 16]); and (ii) an investigation of the threshold for scalarization for different values of  $\beta$  and  $\lambda$  in terms of a simple linear stability criterion, along the

lines of recent work for black holes surrounded by matter [32, 33].

The plan of the paper is as follows. In Section 2 we introduce the equations of motion in scalar-tensor theory and the stress-energy tensor describing anisotropic fluids that will be used in the rest of the paper. In Section 3 we present the equations of structure for relativistic stars at first order in the slow-rotation expansion. The macroscopic properties of NSs obtained by integrating these equations for two different models of anisotropic stars are presented in Section 4. Section 4.3 shows that a linear approximation is sufficient to identify the threshold for spontaneous scalarization for different values of  $\beta$  and  $\lambda$ . Section 5 summarizes our main conclusions and points out possible avenues for future work. Finally, in Appendix A we give a detailed derivation of an integral formula to compute the moment of inertia. Throughout this work, quantities associated with the Einstein (Jordan) frame will be labeled with an asterisk (tilde). We use geometrical units ( $c = G_* = 1$ ) unless stated otherwise and signature  $(-, +, +, +)$ .

## 2. Anisotropic fluids in scalar-tensor theory of gravity

### 2.1. Overview of the theory

We consider a massless scalar-tensor theory described by an Einstein-frame action [27, 42]

$$S = \frac{c^4}{16\pi G_*} \int d^4x \frac{\sqrt{-g_*}}{c} (R_* - 2g_*^{\mu\nu} \partial_\mu \varphi \partial_\nu \varphi) + S_M[\psi_M; A^2(\varphi)g_{*\mu\nu}], \quad (1)$$

where  $G_*$  is the bare gravitational constant,  $g_* \equiv \det[g_{*\mu\nu}]$  is the determinant of the Einstein-frame metric  $g_{*\mu\nu}$ ,  $R_*$  is the Ricci curvature scalar of the metric  $g_{*\mu\nu}$ , and  $\varphi$  is a massless scalar field.  $S_M$  is the action of the matter fields, collectively represented by  $\psi_M$ . Free particles follow geodesics of the Jordan-frame metric  $\tilde{g}_{\mu\nu} \equiv A^2(\varphi)g_{*\mu\nu}$ , where  $A(\varphi)$  is a conformal factor. In this work we assume that  $A(\varphi)$  has the form

$$A(\varphi) \equiv e^{\frac{1}{2}\beta\varphi^2}, \quad (2)$$

where  $\beta$  is the theory's free parameter and, as we recalled in the introduction, current binary pulsar observations constrain it to the range  $\beta \gtrsim -4.5$  [44, 45].

The field equations of this theory, obtained by varying the action  $S$  with respect to  $g_*^{\mu\nu}$  and  $\varphi$ , are given by

$$R_{*\mu\nu} = 2\partial_\mu \varphi \partial_\nu \varphi + 8\pi \left( T_{*\mu\nu} - \frac{1}{2} T_* g_{*\mu\nu} \right), \quad (3)$$

$$\square_* \varphi = -4\pi \alpha(\varphi) T_*, \quad (4)$$

where  $R_{*\mu\nu}$  is the Ricci tensor,  $\alpha(\varphi) \equiv d \log A(\varphi) / d\varphi$  (in the language of [27, 42]) is the ‘‘scalar-matter coupling function’’ and  $\square_*$  is the d'Alembertian operator associated to the metric  $g_{*\mu\nu}$ . GR is obtained in the limit where the scalar field decouples from matter, i.e.  $\alpha(\varphi) \rightarrow 0$ . Under the particular choice of the conformal factor (2), this is equivalent to letting  $\beta = 0$ . In this paper, all equations will be derived within the context of scalar-tensor gravity.

Finally,  $T_*^{\mu\nu}$  is the energy-momentum tensor of the matter fields, defined as

$$T_*^{\mu\nu} \equiv \frac{2}{\sqrt{-g_*}} \frac{\delta S_M[\psi_M, A^2(\varphi)g_{*\mu\nu}]}{\delta g_{*\mu\nu}}, \quad (5)$$

and  $T_* \equiv T_*^{\mu\nu} g_{*\mu\nu}$  is its trace. The energy-momentum tensor in the Jordan frame  $\tilde{T}^{\mu\nu}$ , with trace  $\tilde{T} \equiv \tilde{T}^{\mu\nu} \tilde{g}_{\mu\nu}$ , is defined in an analogous fashion:

$$\tilde{T}^{\mu\nu} \equiv \frac{2}{\sqrt{-\tilde{g}}} \frac{\delta S_M[\psi_M, \tilde{g}_{\mu\nu}]}{\delta \tilde{g}_{\mu\nu}}. \quad (6)$$

The two energy-momentum tensors (and their traces) are related as follows:

$$T_*^{\mu\nu} = A^6(\varphi) \tilde{T}^{\mu\nu}, \quad T_{*\mu\nu} = A^2(\varphi) \tilde{T}_{\mu\nu}, \quad T_* = A^4(\varphi) \tilde{T}. \quad (7)$$

The covariant divergence of the energy-momentum tensor satisfies

$$\nabla_{*\mu} T_*^{\mu\nu} = \alpha(\varphi) T_* \nabla_*^\nu \varphi, \quad (8)$$

$$\tilde{\nabla}_\mu \tilde{T}^{\mu\nu} = 0, \quad (9)$$

in the Einstein and Jordan frames, respectively.

## 2.2. Anisotropic fluids

An anisotropic fluid with radial pressure  $\tilde{p}$ , tangential pressure  $\tilde{q}$  and total energy density  $\tilde{\epsilon}$  can be modeled by the Jordan-frame energy-momentum tensor [15, 46]

$$\tilde{T}_{\mu\nu} = \tilde{\epsilon} \tilde{u}_\mu \tilde{u}_\nu + \tilde{p} \tilde{k}_\mu \tilde{k}_\nu + \tilde{q} \tilde{\Pi}_{\mu\nu}, \quad (10)$$

where  $\tilde{u}_\mu$  is the fluid four-velocity,  $\tilde{k}_\mu$  is a unit radial vector ( $\tilde{k}_\mu \tilde{k}^\mu = 1$ ) satisfying  $\tilde{u}^\mu \tilde{k}_\mu = 0$ , and  $\tilde{\Pi}_{\mu\nu} \equiv \tilde{g}_{\mu\nu} + \tilde{u}_\mu \tilde{u}_\nu - \tilde{k}_\mu \tilde{k}_\nu$ .  $\tilde{\Pi}_{\mu\nu}$  is a projection operator onto a two-surface orthogonal to both  $\tilde{u}_\mu$  and  $\tilde{k}_\mu$ : indeed, defining a projected vector  $\tilde{A}^\mu \equiv \tilde{\Pi}^{\mu\nu} \tilde{V}_\nu$ , one can easily verify that  $\tilde{u}_\mu \tilde{A}^\mu = \tilde{k}_\mu \tilde{A}^\mu = 0$ . At the center of symmetry of the fluid distribution the tangential pressure  $\tilde{q}$  must vanish, since  $\tilde{k}^\mu$  is not defined there [46]. The trace of the Einstein-frame stress-energy tensor for an anisotropic fluid is

$$T_* = A^4(\varphi) [-(\tilde{\epsilon} - 3\tilde{p}) - 2(\tilde{p} - \tilde{q})]. \quad (11)$$

As emphasized by Bowers and Liang [15],  $\tilde{p}$  and  $\tilde{q}$  contain contributions from fluid pressures and other possible stresses inside the star, therefore they should not be confused with purely hydrostatic pressure. Additional stresses could be caused, for instance, by the presence of a solid core [2], strong magnetic fields [3] or a multi-fluid mixture [14]. The derivation of a microphysical model for anisotropy is a delicate issue, so we will adopt a phenomenological approach. We will assume that  $\tilde{p}$  is described by a barotropic EoS, i.e.  $\tilde{p} = \tilde{p}(\tilde{\epsilon})$ . For brevity in this paper we focus on the APR EoS [47], but we have verified that our qualitative results do not depend on this choice. The APR EoS supports NS models with a maximum mass  $M$  larger than  $2.0 M_\odot$ , and therefore it is compatible with the recent observations of the  $M = 1.97 \pm 0.04 M_\odot$  pulsar PSR J1614-2230 [48] and of the  $M = 2.01 \pm 0.04 M_\odot$  pulsar PSR J0348+0432 [49].

The functional form of the anisotropy  $\tilde{\sigma} \equiv \tilde{p} - \tilde{q}$  [15, 46, 50] depends on microscopic relationships between  $\tilde{p}$ ,  $\tilde{q}$  and  $\tilde{\epsilon}$ , that unfortunately are not known. However we can introduce physically motivated functional relations for  $\tilde{\sigma}$  that allow for a smooth transition between the isotropic and anisotropic regimes. Many such functional forms have been studied in the literature. As an application of our general formalism we will consider two of these phenomenological relations, described below.

*2.2.1. Quasi-local equation of state* Horvat et al. [16] proposed the following quasi-local equation for  $\tilde{\sigma}$ :

$$\tilde{\sigma} \equiv \lambda_{\text{H}} \tilde{\rho} \tilde{\gamma}, \quad (12)$$

where  $\tilde{\gamma} \equiv 2\mu(r)/r$ . The ‘‘mass function’’  $\mu(r)$ , defined in Eq. (15) below, is essentially the mass contained within the radius  $r$ , so the quantity  $\tilde{\gamma}$  is a local measure of compactness, whereas  $\lambda_{\text{H}}$  is a free (constant) parameter that controls the degree of anisotropy.

The calculations of [9] show that, if anisotropy occurs due to pion condensation,  $0 \leq \tilde{\sigma}/\tilde{\rho} \leq 1$ , therefore  $\lambda_{\text{H}}$  could be of order unity [46]. More recently, Nelmes and Piette [11] considered NS structure within a model consisting of a Skyrme crystal, which allows for the presence of anisotropic strains. They found that  $\lambda_{\text{H}}$ , as defined in Eq. (12), has a nearly constant value  $\lambda_{\text{H}} \approx -2$  throughout the NS interior. The nonradial oscillations of anisotropic stars were studied in [46] using the model of Eq. (12). Following Doneva and Yazadjiev [46], we will consider values of  $\lambda_{\text{H}}$  in the range  $-2 \leq \lambda_{\text{H}} \leq 2$ .

*2.2.2. Bowers-Liang model* As a second possibility we will consider the functional form for  $\tilde{\sigma}$  proposed by Bowers and Liang [15], who suggested the relation<sup>‡</sup>

$$\tilde{\sigma} \equiv \frac{1}{3} \lambda_{\text{BL}} (\tilde{\epsilon} + 3\tilde{p}) (\tilde{\epsilon} + \tilde{p}) \left(1 - \frac{2\mu}{r}\right)^{-1} r^2. \quad (13)$$

The model is based on the following assumptions: (i) the anisotropy should vanish quadratically at the origin (the necessity for this requirement will become clear in Sec. 3), (ii) the anisotropy should depend nonlinearly on  $\tilde{p}$ , and (iii) the anisotropy is (in part) gravitationally induced. The parameter  $\lambda_{\text{BL}}$  controls the amount of anisotropy in the fluid.

This ansatz was used in [15] to obtain an exact solution for incompressible stars with  $\tilde{\epsilon} = \tilde{\epsilon}_0 = \text{constant}$ . In their simple model, the requirement that equilibrium configurations should have finite central pressure  $\tilde{p}_c$  implies that  $\lambda_{\text{BL}} \geq -2$ . The Newtonian limit of the Bowers-Liang ansatz was also considered in a recent study of the correspondence between superradiance and tidal friction [50]. In our calculations we will assume that  $-2 \leq \lambda_{\text{BL}} \leq 2$ .

### 3. Stellar structure in the slow-rotation approximation

In this Section we approximate the metric of a slowly, rigidly rotating, anisotropic star following the seminal work by Hartle and Thorne [51, 52]. The idea is to consider the effects of rotation as perturbations of the spherically symmetric background spacetime of a static star. We generalize the results of [51, 52] (in GR) and [42] (in scalar-tensor theory) to account for anisotropic fluids up to first order in rotation, so we can study how anisotropy and scalarization affect the moment of inertia of the star and the dragging of inertial frames.

We remark that the moment of inertia  $I$ , the star’s uniform angular velocity  $\Omega$  and the angular momentum  $J \equiv I\Omega$  are the same in the Jordan and Einstein frames (cf. [42, 53]). Therefore, to simplify the notation, we will drop asterisks and tildes on

<sup>‡</sup> The factor of  $1/3$  in Eq. (13) is chosen for convenience. Also, there is a sign difference between our definition of  $\tilde{\sigma}$  and the one in [15]. Our parameter  $\lambda_{\text{BL}}$  is related with the Bowers-Liang (physically equivalent) parameter  $C$  by  $\lambda_{\text{BL}} = -3C$ .

these quantities. Working at order  $\mathcal{O}(\Omega)$ , the line element of a stationary axisymmetric spacetime in the Jordan frame reads

$$d\tilde{s}^2 = A^2(\varphi) \left[ -e^{2\Phi(r)} dt^2 + e^{2\Lambda(r)} dr^2 + r^2 d\theta^2 + r^2 \sin^2 \theta d\phi^2 - 2\omega(r, \theta) r^2 \sin^2 \theta dt d\phi \right], \quad (14)$$

where

$$e^{-2\Lambda(r)} \equiv 1 - \frac{2\mu(r)}{r}, \quad (15)$$

$\mu(r)$  is the mass function and  $\omega(r, \theta) \sim \mathcal{O}(\Omega)$  is the angular velocity acquired by a particle falling from infinity as measured by a static asymptotic observer [51].

The four-velocity of the rotating fluid is such that  $\tilde{u}_\mu \tilde{u}^\mu = -1$ , and it has components [51]

$$\tilde{u}^0 = [-(\tilde{g}_{00} + 2\Omega\tilde{g}_{03} + \Omega^2\tilde{g}_{33})]^{-1/2}, \quad (16)$$

$$\tilde{u}^1 = \tilde{u}^2 = 0, \quad (17)$$

$$\tilde{u}^3 = \Omega\tilde{u}^0. \quad (18)$$

Using (14), at first order in the slow-rotation parameter we obtain:

$$\tilde{u}^\mu = A^{-1}(\varphi) (e^{-\Phi}, 0, 0, \Omega e^{-\Phi}). \quad (19)$$

Following the standard procedure [37, 51, 54], the field equations (3), (4) and (8) with the metric given by (1) yield the following set of ordinary differential equations:

$$\frac{d\mu}{dr} = 4\pi A^4(\varphi) r^2 \tilde{\epsilon} + \frac{1}{2} r(r - 2\mu) \psi^2, \quad (20)$$

$$\frac{d\Phi}{dr} = 4\pi A^4(\varphi) \frac{r^2 \tilde{p}}{r - 2\mu} + \frac{1}{2} r \psi^2 + \frac{\mu}{r(r - 2\mu)}, \quad (21)$$

$$\begin{aligned} \frac{d\psi}{dr} &= 4\pi A^4(\varphi) \frac{r}{r - 2\mu} [\alpha(\varphi)(\tilde{\epsilon} - 3\tilde{p}) + r(\tilde{\epsilon} - \tilde{p})\psi] \\ &\quad - \frac{2(r - \mu)}{r(r - 2\mu)} \psi + 8\pi A^4(\varphi) \alpha(\varphi) \frac{r\tilde{\sigma}}{r - 2\mu}, \end{aligned} \quad (22)$$

$$\frac{d\tilde{p}}{dr} = -(\tilde{\epsilon} + \tilde{p}) \left[ \frac{d\Phi}{dr} + \alpha(\varphi)\psi \right] - 2\tilde{\sigma} \left[ \frac{1}{r} + \alpha(\varphi)\psi \right], \quad (23)$$

$$\begin{aligned} \frac{d\varpi}{dr} &= 4\pi A^4(\varphi) \frac{r^2}{r - 2\mu} (\tilde{\epsilon} + \tilde{p}) \left( \varpi + \frac{4\tilde{\omega}}{r} \right) + \left( r\psi^2 - \frac{4}{r} \right) \varpi \\ &\quad + 16\pi A^4(\varphi) \frac{r\tilde{\sigma}}{r - 2\mu} \tilde{\omega}, \end{aligned} \quad (24)$$

where we defined  $\psi \equiv d\varphi/dr$ ,  $\varpi \equiv d\tilde{\omega}/dr$ , and  $\tilde{\omega} \equiv \Omega - \omega$ . The equations above reduce to the Tolman-Oppenheimer-Volkoff (TOV) equations for anisotropic stars in GR [15] when  $\alpha \rightarrow 0$ , to the results of [27] in the isotropic limit  $\tilde{\sigma} \rightarrow 0$ , and to the usual TOV equations when both quantities are equal to zero [37]. In the GR limit, our frame-dragging equation (24) agrees with Bayin's [21] result §.

§ In principle, as mentioned in the introduction, rotation may induce anisotropy. Therefore the Horvat et al. and Bowers-Liang models for  $\tilde{\sigma}$  should contain terms proportional to  $\Omega$ . However, Eq. (24) implies that such terms in  $\tilde{\sigma}$  would lead to corrections of second order in the angular velocity  $\Omega$ . These corrections are beyond the scope of the  $\mathcal{O}(\Omega)$  approximation considered in our work.

To obtain the interior solution we integrate the generalized TOV equations (20)-(24) from a point  $r_c$  close to the stellar center  $r = 0$  outwards up to a point  $r = r_s$  where the pressure vanishes, i.e.  $\tilde{p}(r_s) = 0$ . This point specifies the Einstein-frame radius  $R_* \equiv r_s$  of the star. If  $\varphi_s = \varphi(r_s)$ , the Jordan-frame radius  $\tilde{R}$  is

$$\tilde{R} = A(\varphi_s) R_*. \quad (25)$$

In practice, to improve numerical stability, given  $\tilde{\epsilon}_c$ ,  $\Phi_c$ ,  $\varphi_c$  and  $\mu_c$  (where the subscript c means that all quantities are evaluated at  $r = 0$ ) we use the following series expansions:

$$\begin{aligned} \mu &= \frac{4}{3}\pi A_c^4 \tilde{\epsilon}_c r^3 + \mathcal{O}(r^4), \\ \Phi &= \Phi_c + \frac{2}{3}\pi A_c^4 (\tilde{\epsilon}_c + 3\tilde{p}_c) r^2 + \mathcal{O}(r^4), \\ \tilde{p} &= \tilde{p}_c + \frac{2}{3}\pi r^2 A_c^4 (\tilde{\epsilon}_c + \tilde{p}_c) [3\tilde{p}_c (\alpha_c^2 - 1) - \tilde{\epsilon}_c (\alpha_c^2 + 1)] + \\ &\quad - \frac{1}{3}r^2 (2r\sigma_3 + 3\sigma_2) + \mathcal{O}(r^4), \\ \varphi &= \varphi_c + \frac{2\pi}{3} A_c^4 \alpha_c (\tilde{\epsilon}_c - 3\tilde{p}_c) r^2 + \mathcal{O}(r^4), \\ \bar{\omega} &= \bar{\omega}_c + \frac{8\pi}{5} A_c^4 \bar{\omega}_c (\tilde{\epsilon}_c + \tilde{p}_c) r^2 + \mathcal{O}(r^4), \\ \tilde{\sigma} &= \sigma_2 r^2 + \sigma_3 r^3 + \mathcal{O}(r^4), \end{aligned} \quad (26)$$

where  $\sigma_2$  and  $\sigma_3$  depend on the particular anisotropy model.

In the vacuum exterior we have  $\tilde{p} = \tilde{\epsilon} = \tilde{\sigma} = 0$ . Eqs. (20)-(22) must be integrated outwards starting from the stellar radius to obtain the stellar mass, angular momentum and scalar charge. For large  $r$  we can expand the relevant functions as follows:

$$\mu(r) = M - \frac{Q^2}{2r} - \frac{MQ^2}{2r^2} + \mathcal{O}(r^{-3}) \quad (27)$$

$$e^{2\Phi} = 1 - \frac{2M}{r} + \mathcal{O}(r^{-3}), \quad (28)$$

$$\varphi(r) = \varphi_\infty + \frac{Q}{r} + \frac{MQ}{r^2} + \mathcal{O}(r^{-3}), \quad (29)$$

$$\bar{\omega}(r) = \Omega - \frac{2J}{r^3} + \mathcal{O}(r^{-4}), \quad (30)$$

where  $M$  is the Arnowitt-Deser-Misner (ADM) mass of the NS,  $Q$  is the scalar charge,  $J$  is the star's angular momentum and  $\varphi_\infty$  is the (constant) cosmological value of the scalar field, here assumed to be zero. Under this assumption the mass  $M$  is the same in the Jordan and Einstein frames [53]. By matching the numerical solution integrated from the surface of the star with the asymptotic expansions (27)-(30) we can compute  $M$ ,  $Q$  and  $J$ .

We compute the moment of inertia of the star  $I$  in two equivalent ways. The first method consists of extracting the angular momentum as described above and using

$$I = \frac{J}{\Omega}. \quad (31)$$

In alternative, we can compute  $I$  through an integral within the star. Combining Eqs. (15), (20)-(21) and (24) we obtain the following integral expression:

$$I = \frac{8\pi}{3} \int_0^{R_*} A^4(\varphi) e^{\Lambda - \Phi} r^4 (\tilde{\epsilon} + \tilde{p}) \left(1 - \frac{\tilde{\sigma}}{\tilde{\epsilon} + \tilde{p}}\right) \left(\frac{\bar{\omega}}{\Omega}\right) dr \quad (32)$$

(see Appendix A for details). As  $A(\varphi) \rightarrow 1$  and  $\tilde{\sigma} \rightarrow 0$  we recover Hartle's result [51], and in the isotropic limit  $\tilde{\sigma} \rightarrow 0$  we match the result of [54]. The numerical values of  $I$  obtained with (31) and (32) are in excellent agreement.

For each stellar model we also calculate the *baryonic mass*  $\tilde{M}_b$ , defined as [27]

$$\tilde{M}_b \equiv 4\pi\tilde{m}_b \int_0^{R_*} \tilde{n} A^3(\varphi) \frac{r^2}{\sqrt{1-2\mu/r}} dr, \quad (33)$$

where  $\tilde{m}_b = 1.66 \times 10^{-24}$  g is the atomic mass unit and  $\tilde{n}$  is the baryonic number density.

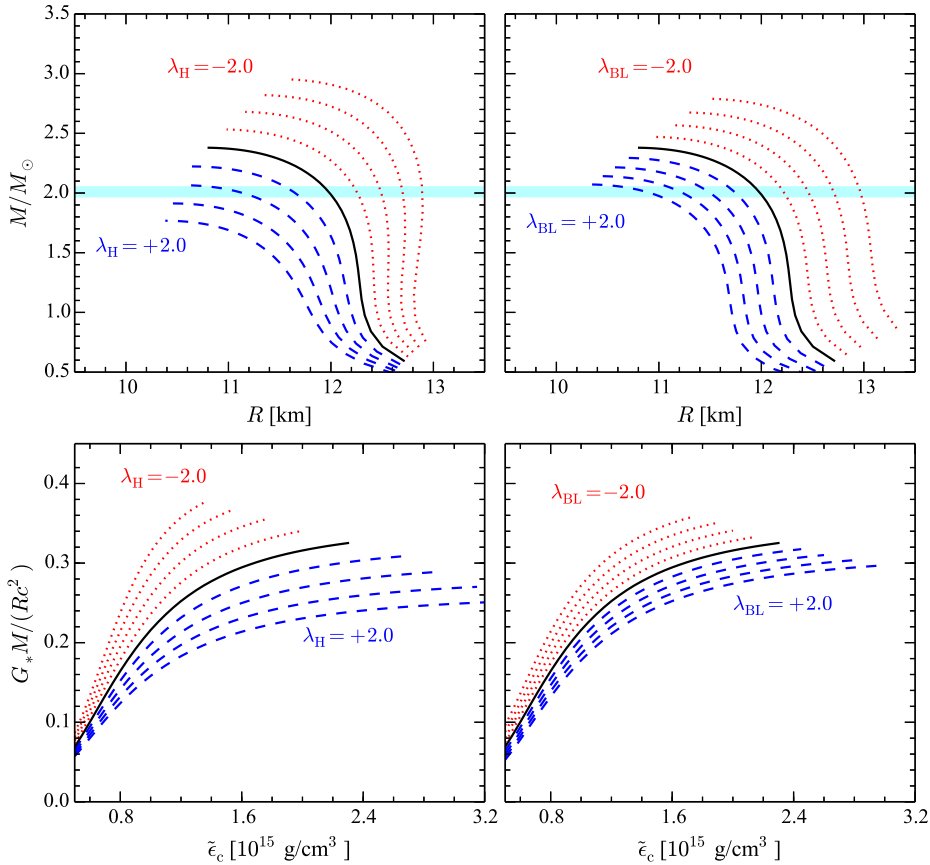


**Figure 1.** Mass-radius relation (top panels) and dimensionless compactness  $G_*M/Rc^2$  as a function of the central density (bottom panels) for anisotropic stars in GR using EoS APR. In the left panels we use the quasi-local model of [16]; in the right panels, the Bowers-Liang model [15]. Different curves correspond to increasing  $\lambda_H$  (or  $\lambda_{BL}$ ) in increments of 0.5 between  $-2$  (top) and  $2$  (bottom). The shaded blue bar corresponds to the mass  $M = 2.01 \pm 0.04 M_\odot$  of PSR J0348+0432 [49].



## 4. Numerical results

The tools developed so far allow us to investigate the effect of anisotropy on the bulk properties of rotating stars. In Section 4.1 we will focus on slowly rotating stars in GR. To the best of our knowledge – and to our surprise – rotating anisotropic stars have not been studied in the GR literature, with the only exception of a rather mathematical paper by Bayin [21]. In Section 4.2 we extend our study to scalar-tensor theories. Our main motivation here is to understand whether anisotropy may increase the critical value  $\beta = \beta_{\text{crit}}$  above which spontaneous scalarization cannot happen, and therefore allow for observationally interesting modifications to the structure of NSs that would still be compatible with the stringent bounds from binary pulsars [44, 45].

### 4.1. The effect of anisotropy in GR

In the top panels of Figure 1 we show the mass-radius relation for anisotropic NS models in GR. All curves are truncated at the central density corresponding to the maximum NS mass, because models with larger central densities are unstable to radial perturbations [36, 37]. Solid lines correspond to  $\tilde{\sigma} = 0$ , i.e. the isotropic fluid limit. The horizontal shaded band in the upper panels represents the largest measured NS mass  $M = 2.01 \pm 0.04 M_{\odot}$  (PSR J0348+0432: cf. [49]).

Recall that  $\tilde{\sigma} = \tilde{p} - \tilde{q}$  is proportional to  $\lambda_{\text{H}}$  and  $\lambda_{\text{BL}}$  (with a positive proportionality constant) in both models, and that  $\tilde{p}$  and  $\tilde{q}$  represent the “radial” and “tangential” pressures, respectively. Therefore positive values of  $\lambda_{\text{H}}$  and  $\lambda_{\text{BL}}$  mean that the radial pressure is larger than the tangential pressure (dashed lines); the opposite is true when the anisotropy parameters are negative (dotted lines).

The trend in the top panels of Figure 1 is clear: for both anisotropy models, positive (negative) anisotropy parameters yield smaller (larger) radii at fixed mass, and smaller masses at fixed radius. The lower panels of Figure 1 show that the stellar compactness  $G_*M/(Rc^2)$  decreases (for a given EoS and fixed central density) as the anisotropy degree increases. Nuclear matter EoSs are usually ordered in terms of a “stiffness” parameter, with stiffer EoSs corresponding to larger sound speeds (more incompressible matter) in the stellar interior, and larger values of the compactness  $M/R$ . The qualitative effect of increasing anisotropy (with our sign conventions) is *opposite* (for a given EoS) to the qualitative effect of increasing stiffness.

Figure 2 is, to our knowledge, the first calculation of the effect of anisotropy on the moment of inertia  $I$ . As in Figure 1, solid lines corresponds to the isotropic limit. In the right panel we use the quasi-local model of [16]; in the left panel, the Bowers-Liang model [15]. Hypothetical future observations of the moment of inertia of star A, from the double pulsar PSR J0737-3039 [55, 56, 57], or preferably from large-mass NSs, may be used to constrain the degree of anisotropy under the assumptions that GR is valid and that the nuclear EoS is known.

### 4.2. The effect of anisotropy on spontaneous scalarization

In Figures 3 and 4 we display the properties of nonrotating, spontaneously scalarized stars within the anisotropy models of Horvat et al. [16] and Bowers-Liang [15], respectively. The main panel in each Figure shows the mass-radius relation as the anisotropy parameter increases (in increments of 1, and from top to bottom) in the range  $-2 \leq \lambda_{\text{H}} \leq 2$  (Figure 3) or  $-2 \leq \lambda_{\text{BL}} \leq 2$  (Figure 4). Solid lines correspond to the GR limit; dotted, dashed and dash-dotted lines correspond to  $\beta = -4.3$ ,  $-4.4$

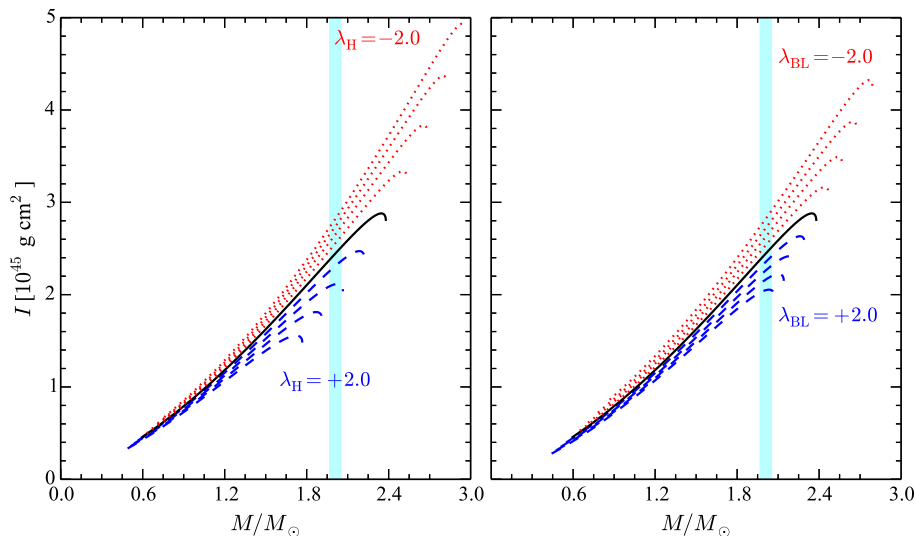


**Figure 2.** The moment of inertia  $I$  as function of the mass  $M$  for anisotropic stars in GR using EoS APR, increasing  $\lambda_H$  (or  $\lambda_{BL}$ ) in increments of 0.5 between  $-2$  (top curves) and  $2$  (bottom curves). As in Figure 1, the vertical shaded region marks the largest measured NS mass [49].

and  $-4.5$ , as indicated in the legend. The lower panels show the scalar charge  $Q/M$  as a function of the baryonic mass. In each of these panels we plot the scalar charge for a fixed value of  $\beta$  and different anisotropy parameters.

For isotropic EoSs in GR, Harada [43] used catastrophe theory to show that scalarization is only possible when  $\beta \lesssim -4.35$ . We find that scalarization can occur for larger values of  $\beta$  in the presence of anisotropy. For example, for a value of  $\lambda_H \sim -2$  (compatible with the Skyrme model predictions of [11]) scalarization is possible when  $\beta \simeq -4.15$ , and for  $\beta \simeq -4.3$  scalarization produces rather large ( $\approx 10\%$ ) deviations in the mass-radius relation. This qualitative conclusion applies to both anisotropy models considered by us. The lower panels show that: (i) for fixed  $\beta$  (i.e., for a fixed theory) and for a fixed central density, the “strength” of scalarization – as measured by the scalar charge of the star – increases for large negative  $\lambda$ ’s, i.e. when the tangential pressure is significantly larger than the radial pressure, for both anisotropy models; (ii) scalarization occurs in a much wider range of baryonic masses, all of which are compatible with the range where anisotropy would be expected according to the Skyrme model predictions of [11]. These calculations are of course preliminary and should be refined using microphysical EoS models. However, let us remark once again that the scalarization threshold in the absence of anisotropy is to a very good approximation EoS-independent, and stars only acquire significant scalar charge when  $\beta < -4.35$  (as shown in [43] and in Figure 6 below). In the admittedly unlikely event that binary pulsar observations were to hint at scalarization with  $\beta > -4.35$ , this would be strong evidence for the presence of anisotropy<sup>||</sup> and even lead to experimental

<sup>||</sup> An important caveat here is that *fast* rotation can also strengthen the effects of scalarization: according to [58], scalarization can occur for  $\beta < -3.9$  for NSs spinning at the mass-shedding limit. However the NSs found in binary pulsar systems are relatively old, as they are expected to be spinning well below the mass-shedding limit, where the slow-rotation approximation works very well [59].

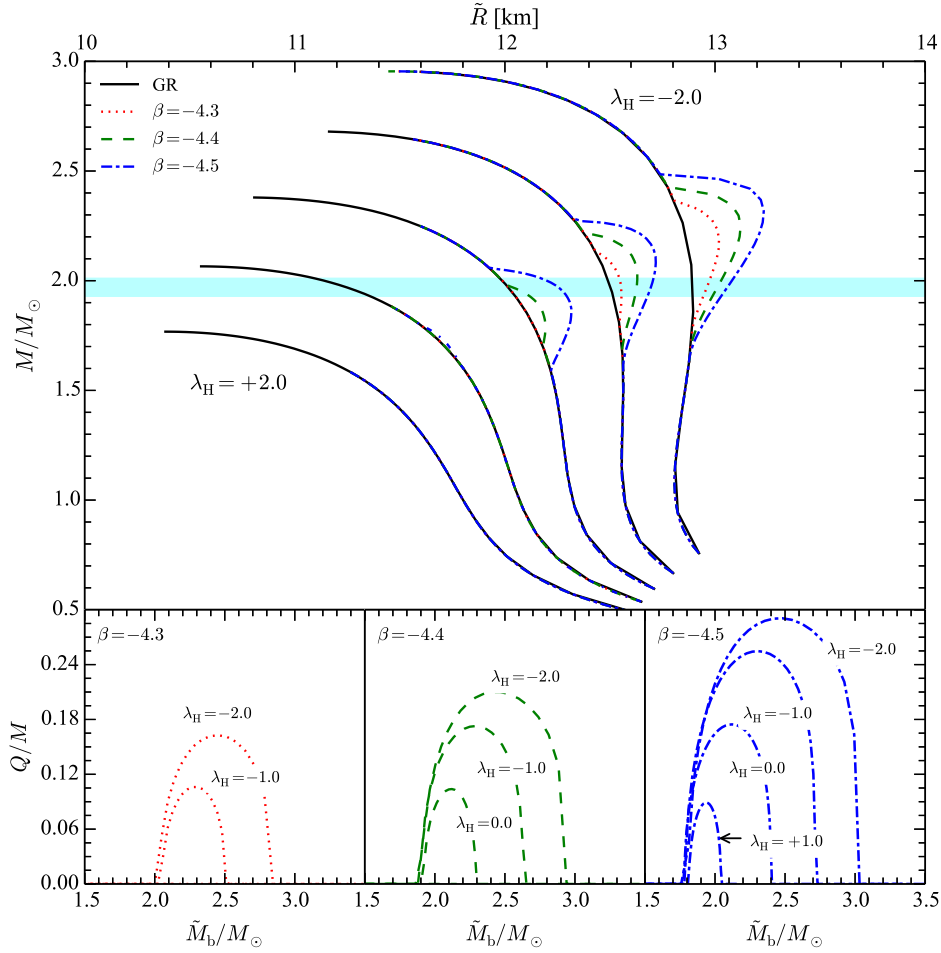


**Figure 3.** Spontaneous scalarization in the quasi-local model of Horvat et al. [16]. See the main text for details.

constraints on the Skyrme model and QCD.

As in Figure 2, in the left panel of Figure 5 we show the moment of inertia as a function of the stellar mass for the quasi-local model of [16], while the right panel refers to the Bowers-Liang model [15]. Solid lines corresponds to the GR limit for different anisotropy parameters. Unsurprisingly, the largest modifications to the moment of inertia occur for large negative  $\lambda$ 's, and they follow the same trends highlighted in our discussion of the mass-radius relation.

#### 4.3. Critical scalarization point in the linearized approximation

The condition for spontaneous scalarization to occur can be found in a linearized approximation to the scalar-field equation of motion. The idea is that *at the onset* of

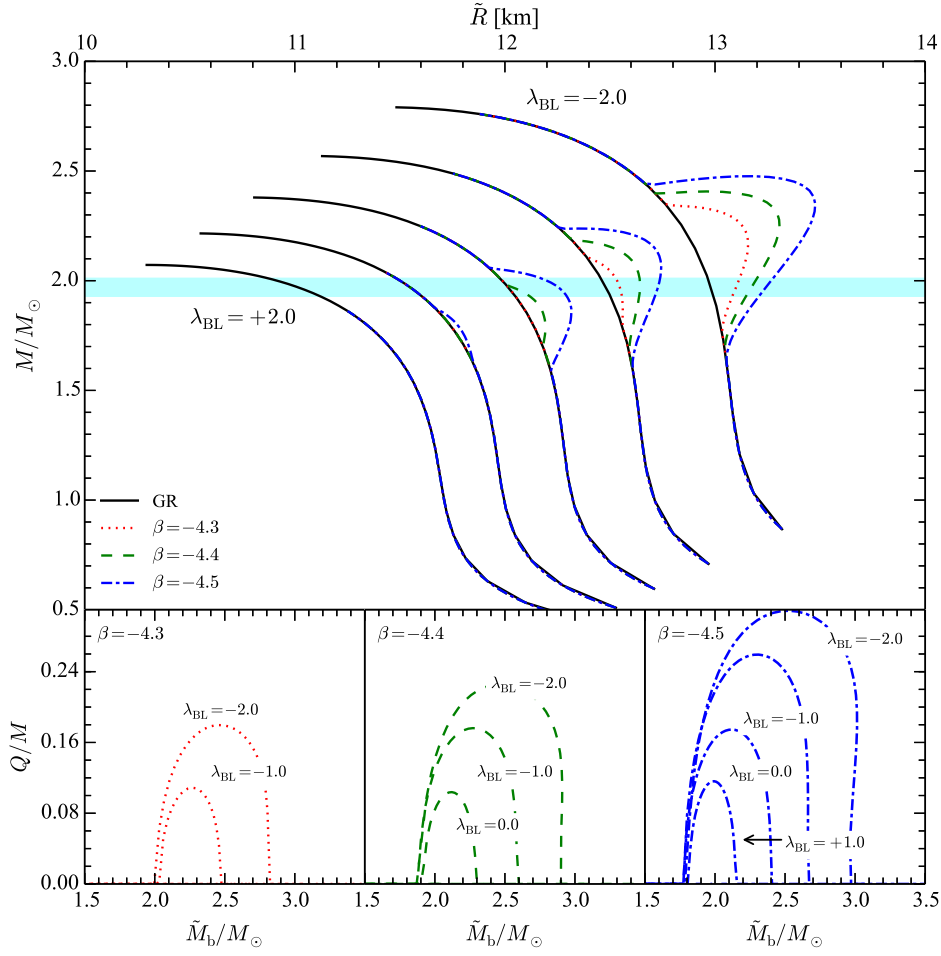


**Figure 4.** Same as Figure 3, but for the Bowers-Liang anisotropy model [15].

scalarization the scalar field must be small, so we can neglect its backreaction on the geometry and look for bound states of the scalar field by dropping terms quadratic in the field [27, 42]. Here we study general conditions for the existence of bound states in the linearized regime, and we show that (as expected based on the previous argument) the linearized theory does indeed give results in excellent agreement with the full, nonlinear calculation.

Redefining the scalar field as  $\varphi(t, r) = r^{-1}\Psi(r)e^{-i\nu t}$  and neglecting terms  $\mathcal{O}(\varphi^2)$ , Eq. (4) can be written as a Schrödinger-like equation:

$$\frac{d^2\Psi}{dx^2} + [\nu^2 - V_{\text{eff}}(x)]\Psi = 0, \quad (34)$$

where the tortoise radial coordinate  $x$  is defined by  $dx \equiv dr e^{-\Phi}/\sqrt{1-2\mu/r}$ . The

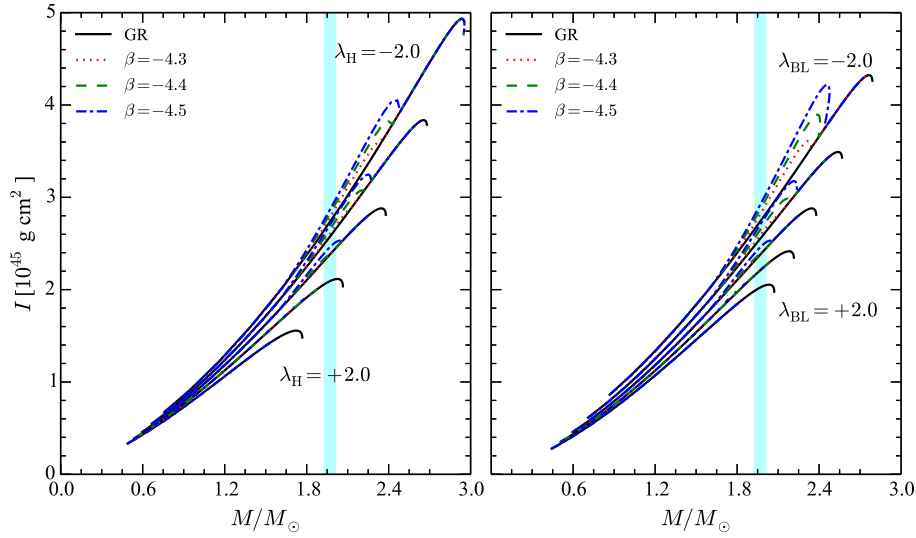


**Figure 5.** Same as Figure 2, but in scalar-tensor theories with different values of  $\beta$ .

effective potential is

$$V_{\text{eff}}(r) \equiv e^{2\Phi} \left[ \mu_{\text{eff}}^2(r) + \frac{2\mu}{r^3} + 4\pi(\tilde{p} - \tilde{\epsilon}) \right], \quad (35)$$

where we have introduced an effective (position-dependent) mass

$$\mu_{\text{eff}}^2(r) \equiv -4\pi\beta T_*. \quad (36)$$

Eq. (34) with the potential (35) is a wave equation for a scalar field with effective mass  $\mu_{\text{eff}}$ . From Eq. (11) we see that anisotropy affects the effective mass (and therefore the scalarization threshold) because  $T_*$  contains a term proportional to  $\tilde{\sigma}$ , that in turn is proportional to either  $\lambda_H$  or  $\lambda_{BL}$ : cf. Eqs. (12) and (13). The case of spontaneous scalarization around black holes (studied in [32, 33]) can be recovered by setting  $\tilde{\epsilon} = \tilde{p} = 0$ .

The scalarization threshold can be analyzed by looking for the zero-energy ( $\nu \sim 0$ ) bound state solutions of Eq. (34). In this case, the scalar field satisfies the following boundary conditions:

$$\Psi \sim \begin{cases} \varphi_c r & \text{as } r \rightarrow 0, \\ \varphi_\infty & \text{as } r \rightarrow \infty, \end{cases} \quad (37)$$

and we impose  $\Psi'(r \rightarrow \infty) = 0$ , where the prime denotes derivative with respect to  $r$ . To obtain the scalarization threshold we integrate Eq. (34) outwards, starting from  $r = 0$ , with the above boundary conditions. Since the equation is linear,  $\varphi_c$  is arbitrary. At infinity we impose that the first derivative of  $\Psi$  with respect to  $r$  must be zero. This is a two-point boundary value problem that can be solved with a standard shooting method to find the critical value of the central density  $\tilde{\epsilon}_c$  for which the above conditions are satisfied, given fixed values of  $\beta$  and  $\lambda_H$  (or  $\lambda_{BL}$ ). The solution is some

$$\tilde{\epsilon}_i = \tilde{\epsilon}_i(\beta), \quad (38)$$

where  $\tilde{\epsilon}_i$  is the smallest critical density at which scalarization can occur for the given  $\beta$ . The largest critical density producing scalarization can be similarly obtained by looking for zero-energy bound state solutions to find some

$$\tilde{\epsilon}_f = \tilde{\epsilon}_f(\beta). \quad (39)$$

It can be shown that in these two regimes (i.e., at the starting and ending points of the scalarization regime) the derivative of  $\Psi'(r \rightarrow \infty)$  with respect to  $\tilde{\epsilon}_c$  has opposite signs:

$$\frac{\partial}{\partial \tilde{\epsilon}_c} \Psi'(r \rightarrow \infty) \begin{cases} < 0 & \text{for } \tilde{\epsilon}_c = \tilde{\epsilon}_i, \\ > 0 & \text{for } \tilde{\epsilon}_c = \tilde{\epsilon}_f. \end{cases} \quad (40)$$

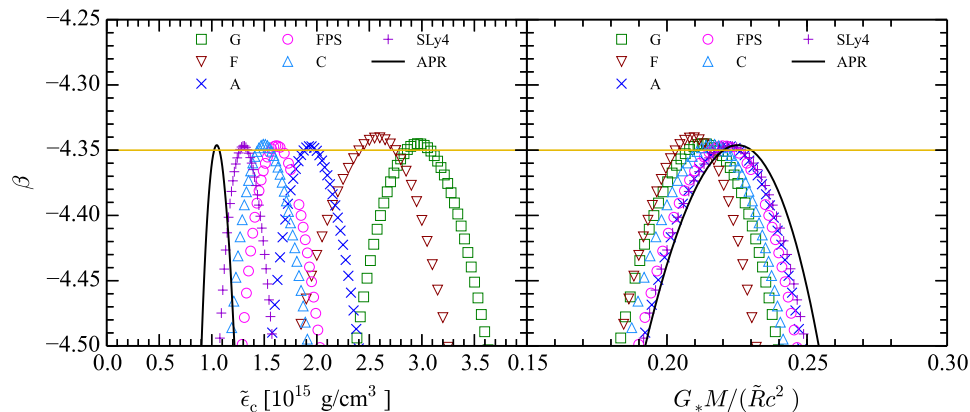


**Figure 6.** Critical  $\beta$  for scalarization as a function of the central density (left panel) and of the stellar compactness (right panel) for nonrotating NS models constructed using different nuclear-physics based EoSs, in the absence of anisotropy.

As a warm-up, in Figure 6 we compute the scalarization threshold for nonrotating isotropic stars with several nuclear-physics based EoSs. The original references for the subset of EoSs used here can be found in [60] (the one exception is SLy4: cf. [61]). The EoSs are sorted by stiffness, with APR EoS being the stiffest and G EoS the softest in our catalog. As a trend, for stiffer EoSs scalarization occurs at lower values of the central densities and at higher values of the compactness. The most remarkable fact is that the value  $\beta = \beta_{\max}$  above which scalarization cannot occur is very narrow: it ranges from  $\beta_{\max} = -4.3462$  for APR EoS to  $\beta_{\max} = -4.3405$  for F EoS [62]. This is consistent with Harada’s study based on catastrophe theory, that predicts a threshold value  $\beta_{\max} \simeq -4.35$  (horizontal line in the figure) in the absence of anisotropy [43] (see also [63]).

In Table 1 we compare the values for  $\tilde{\epsilon}_i$  and  $\tilde{\epsilon}_f$  computed using (i) the linearized method described in this Section, and (ii) the full nonlinear set of equations for anisotropic models constructed using the APR EoS. The results agree remarkably well, showing that the onset of scalarization can be analyzed to an excellent degree of accuracy by neglecting the backreaction effects of the scalar field on the geometry. The last column of Table 1 lists  $\beta_{\max}$ , the value of  $\beta$  above which scalarization cannot happen. We do not present results for  $\lambda_H = 2$  because the resulting  $\beta_{\max}$  is already ruled out by binary pulsar observations [44].

**Table 1.** Critical density values obtained through the linearized theory and the full nonlinear equations for APR EoS, different values of the Horvat et al. anisotropy parameter  $\lambda_H$  and  $\beta = -4.5$ : for these choices of parameters, the solution is scalarized if  $\tilde{\epsilon}_i < \tilde{\epsilon}_c < \tilde{\epsilon}_f$ . The last column lists the critical value  $\beta = \beta_{\max}$  above which scalarization is not possible.

$\lambda_H$	Linearized		Full nonlinear		$\beta_{\max}$
	$\tilde{\epsilon}_i (\text{g cm}^{-3})$	$\tilde{\epsilon}_f (\text{g cm}^{-3})$	$\tilde{\epsilon}_i (\text{g cm}^{-3})$	$\tilde{\epsilon}_f (\text{g cm}^{-3})$	
-2	$6.983 \times 10^{14}$	$9.141 \times 10^{14}$	$6.980 \times 10^{14}$	$9.140 \times 10^{14}$	-4.150
-1	$7.819 \times 10^{14}$	$1.053 \times 10^{15}$	$7.817 \times 10^{14}$	$1.053 \times 10^{15}$	-4.239
0	$9.021 \times 10^{14}$	$1.216 \times 10^{15}$	$9.021 \times 10^{14}$	$1.216 \times 10^{15}$	-4.346
1	$1.127 \times 10^{15}$	$1.340 \times 10^{15}$	$1.126 \times 10^{15}$	$1.341 \times 10^{15}$	-4.471

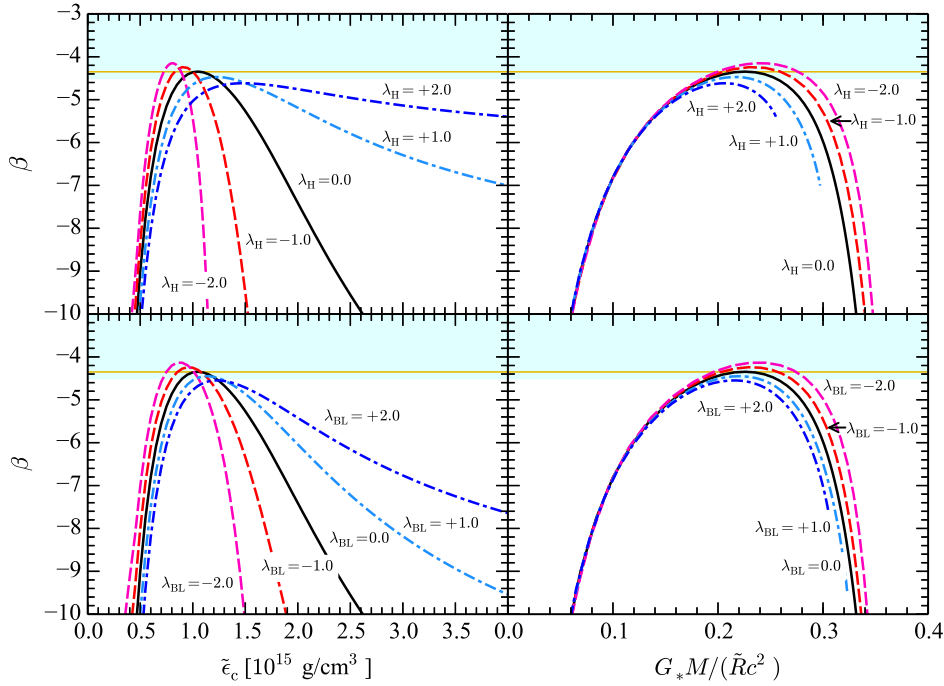


**Figure 7.** Left panels:  $\beta$  versus critical central densities for different values of  $\lambda_{H,BL}$ . Right panels:  $\beta$  versus compactness  $G_*M/\tilde{R}c^2$  of the critical solutions for different values of  $\lambda_{H,BL}$ .

In the left panels of Figure 7 we analyze the dependence of the critical  $\beta$  on the central density, focusing on EoS APR and selecting different values of the anisotropy parameters  $\lambda_{BL}$  (top) and  $\lambda_H$  (bottom). The shaded region at the top ( $\beta \gtrsim -4.5$ ) is allowed by current binary pulsar observations [44, 45]. The horizontal line is the roughly EoS-independent threshold  $\beta_{\max} \simeq -4.35$  for isotropic stars. For a given theory, the starting and ending points of the scalarization regime are those for which a  $\beta = \text{constant}$  (horizontal) line crosses the curves. Anisotropic models have two distinctive features: (1) when the tangential pressure is larger than the radial pressure (dashed lines in Figure 7) scalarization can occur even for  $\beta \geq -4.35$  (for example, for the Horvat et al. model with  $\lambda_H = -2$  we have  $\beta_{\text{crit}} = -4.1513$ , and for the

Bowers-Liang model with  $\lambda_{\text{BL}} = -2$  we have  $\beta_{\text{crit}} = -4.1354$ ; cf. Table 1, Figure 4 and Figure 3); (2) when the tangential pressure is smaller than the radial pressure (dash-dotted lines in Figure 7) scalarized solutions may exist for a much wider range of  $\tilde{\epsilon}_c$ .

In the right panels of Figure 7 we plot the critical  $\beta$  as a function of the stellar compactness  $G_*M/\tilde{R}c^2$ . For low compactness ( $M/\tilde{R} \lesssim 0.15$ ) all curves have the same behaviour regardless of  $\lambda_{\text{H}}$  or  $\lambda_{\text{BL}}$ . This universality has two reasons: (1) all modern nuclear-physics based EoS have the same Newtonian limit (cf. [64] for an analytic treatment of this regime for constant density stars); (2) for any given EoS, the effects of anisotropy are suppressed in the Newtonian regime, where pressures and densities are low and the local compactness parameter is small: cf. Eqs. (12) and (13).

## 5. Conclusions

Binary pulsar observations require  $\beta \gtrsim -4.5$  [44, 45], and even more stringent constraints are expected in the near future. As shown in Figure 6, most “ordinary” nuclear-physics based EoSs for nuclear matter predict that scalarization can only occur for  $\beta < \beta_{\text{max}} = -4.35$ . As binary pulsar observations get closer and closer to the limit  $\beta \gtrsim -4.35$ , the spontaneous scalarization mechanism originally proposed by Damour and Esposito-Farèse [27, 42] looks more and more unlikely to be realized in Nature if neutron stars are isotropic.

The admittedly unlikely event of a binary-pulsar observation of scalarization with  $\beta > -4.35$  would be strong evidence for the presence of anisotropy, and it may even lead to experimental constraints on the Skyrme model and QCD. An important caveat here is that *fast* rotation can also strengthen the effects of scalarization: according to [58], scalarization can occur for  $\beta < -3.9$  when NSs spin at the mass-shedding limit. However the NSs found in binary pulsar systems are relatively old, are they are expected to spin well below the mass-shedding limit, where the slow-rotation approximation works very well [59].

Our work can be extended in several directions. An obvious extension is to consider the effects of anisotropy at second or higher order in the Hartle-Thorne expansion. This would allow us to assess whether the recently discovered “I-Love-Q” and “three-hair” universal relations between the multipole moments of the spacetime hold in the presence of anisotropy *and* scalarization [65, 66, 67, 68, 53]. A second obvious extension could consider fast rotating, anisotropic stars (cf. [58, 69]) and the orbital and epicyclic frequencies around these objects [70].

Anisotropy can lower the threshold for scalarization to occur, and this could be of interest to test scalar-tensor theories through gravitational-wave asteroseismology [71, 72, 73]. We also remark that our study used simplified, phenomenological models for anisotropy, when of course it would be desirable to study realistic microphysical models. Last but not least, our study should be extended to evaluate the stellar sensitivities [74, 75] and to identify exclusion regions in the  $(\beta, \lambda)$  parameter space using binary pulsar observations (cf. e.g. [76]).

## Acknowledgments

We are grateful to K. Glampedakis, M. Horbatsch and G. Pappas for discussions, and to G. Pappas for providing EoS data tables. H. O. S. and E. B. were supported by NSF CAREER Grant No. PHY-1055103. C. F. B. M and L. C. B. C would like to thank the



Conselho Nacional de Desenvolvimento Científico e Tecnológico (CNPq), Coordenação de Aperfeiçoamento de Pessoal de Nível Superior (CAPES), and Fundação Amazônia de Amparo a Estudos e Pesquisas do Pará (FAPESPA) for partial financial support. The authors also acknowledge support from the FP7-PEOPLE-2011-IRSES Grant No.295189. The figures were created using the PYTHON-based library MATPLOTLIB [77].

### A. Derivation of equation (32)

In this Appendix we present a derivation of the integral (32), used to compute the moment of inertia  $I$  of slowly rotating stars in scalar-tensor theory. We begin by noting that

$$\frac{d\Lambda}{dr} = \frac{r}{r-2\mu} \left( \frac{1}{r} \frac{d\mu}{dr} - \frac{\mu}{r^2} \right), \quad (\text{A.1})$$

where Eq. (15) implies that  $\Lambda = -(1/2) \log(1 - 2\mu/r)$  and where  $d\mu/dr$  is given by Eq. (20). Introducing the auxiliary variable  $j \equiv e^{-\Phi-\Lambda}$  we find, using Eqs. (21) and (A.1), that

$$\frac{dj}{dr} = -j \left[ 4\pi A^4(\varphi) \frac{r^2}{r-2\mu} (\tilde{\epsilon} + \tilde{p}) + r\psi^2 \right]. \quad (\text{A.2})$$

Multiplying the frame dragging equation (24) by  $j$  and rearranging, we obtain

$$\frac{1}{r^4} \frac{d}{dr} \left( r^4 j \frac{d\bar{\omega}}{dr} \right) = 16\pi A^4(\varphi) \frac{j r^2}{r-2\mu} (\tilde{\epsilon} + \tilde{p}) \left( 1 - \frac{\tilde{\sigma}}{\tilde{\epsilon} + \tilde{p}} \right) \frac{\bar{\omega}}{r}. \quad (\text{A.3})$$

If we multiply by  $r^4$ , integrate from  $r = 0$  to infinity and use the fact that

$$j = 1 + \mathcal{O}(r^{-1}), \quad \text{and} \quad \frac{d\bar{\omega}}{dr} = \frac{6I\Omega}{r^4} + \mathcal{O}(r^{-5}). \quad (\text{A.4})$$

as  $r \rightarrow \infty$ , we finally get Eq. (32).

### References

- [1] Herrera L and Santos N O 1997 *Phys. Rep.* **286** 53–130
- [2] Kippenhahn R and Weigert A 1990 *Stellar structure and evolution* Astronomy and astrophysics library (Springer) ISBN 9783540502111
- [3] Yazadjiev S S 2012 *Phys. Rev. D* **85**(4) 044030
- [4] Folomeev V and Dzhunushaliev V 2015 *Phys.Rev.* **D91** 044040 (*Preprint* [1501.06275](#))
- [5] Kamiab F, Broderick A E and Afshordi N 2015 (*Preprint* [1503.03898](#))
- [6] Heiselberg H and Hjorth-Jensen M 2000 *Phys.Rept.* **328** 237–327 (*Preprint* [nucl-th/9902033](#))
- [7] Ruderman M 1972 *Ann.Rev.Astron.Astrophys.* **10** 427–476
- [8] Canuto V and Chitre S 1974 *Phys.Rev.* **D9** 1587–1613
- [9] Sawyer R 1972 *Phys.Rev.Lett.* **29** 382–385
- [10] Carter B and Langlois D 1998 *Nucl.Phys.* **B531** 478–504 (*Preprint* [gr-qc/9806024](#))
- [11] Nelmes S and Piette B 2012 *Phys.Rev.* **D85** 123004 (*Preprint* [1204.0910](#))
- [12] Adam C, Naya C, Sanchez-Guillen J, Vazquez R and Wereszczynski A 2015 *Phys.Lett.* **B742** 136–142 (*Preprint* [1407.3799](#))
- [13] Adam C, Naya C, Sanchez-Guillen J, Vazquez R and Wereszczynski A 2015 (*Preprint* [1503.03095](#))
- [14] Letelier P S 1980 *Phys. Rev. D* **22**(4) 807–813
- [15] Bowers R L and Liang E P T 1974 *ApJ* **188** 657
- [16] Horvat D, Ilijic S and Marunovic A 2011 *Class.Quant.Grav.* **28** 025009 (*Preprint* [1010.0878](#))
- [17] Dev K and Gleiser M 2003 *Gen.Rel.Grav.* **35** 1435–1457 (*Preprint* [gr-qc/0303077](#))
- [18] Cattoen C, Faber T and Visser M 2005 *Class.Quant.Grav.* **22** 4189–4202 (*Preprint* [gr-qc/0505137](#))

- [19] Schunck F and Mielke E 2003 *Class.Quant.Grav.* **20** R301–R356 (*Preprint* [0801.0307](#))
- [20] Macedo C F, Pani P, Cardoso V and Crispino L C B 2013 *Phys.Rev.* **D88** 064046 (*Preprint* [1307.4812](#))
- [21] Bayin S S 1982 *Phys.Rev.* **D26** 1262
- [22] Fujii Y and Maeda K I 2003 *The Scalar-Tensor Theory of Gravitation* (Cambridge University Press)
- [23] Sotiriou T P and Faraoni V 2010 *Rev. Mod. Phys.* **82** 451–497 arXiv:0805.1726 [gr-qc]
- [24] De Felice A and Tsujikawa S 2010 *Living Rev.Rel.* **13** 3 (*Preprint* [1002.4928](#))
- [25] Will C M 2006 *Living Reviews in Relativity* **9** URL <http://www.livingreviews.org/lrr-2006-3>
- [26] Damour T and Esposito-Farèse G 1992 *Class.Quant.Grav.* **9** 2093–2176
- [27] Damour T and Esposito-Farèse G 1993 *Phys.Rev.Lett.* **70** 2220–2223
- [28] Berti E, Barausse E, Cardoso V, Gualtieri L, Pani P *et al.* 2015 (*Preprint* [1501.07274](#))
- [29] Sotiriou T P and Faraoni V 2012 *Phys.Rev.Lett.* **108** 081103 (*Preprint* [1109.6324](#))
- [30] Stefanov I Z, Yazadjiev S S and Todorov M D 2008 *Mod.Phys.Lett.* **A23** 2915–2931 (*Preprint* [0708.4141](#))
- [31] Doneva D D, Yazadjiev S S, Kokkotas K D and Stefanov I Z 2010 *Phys.Rev.* **D82** 064030 (*Preprint* [1007.1767](#))
- [32] Cardoso V, Carucci I P, Pani P and Sotiriou T P 2013 *Phys.Rev.* **D88** 044056 (*Preprint* [1305.6936](#))
- [33] Cardoso V, Carucci I P, Pani P and Sotiriou T P 2013 *Phys.Rev.Lett.* **111** 111101 (*Preprint* [1308.6587](#))
- [34] Horbatsch M and Burgess C 2012 *JCAP* **1205** 010 (*Preprint* [1111.4009](#))
- [35] Berti E, Cardoso V, Gualtieri L, Horbatsch M and Spherhake U 2013 *Phys.Rev.* **D87** 124020 (*Preprint* [1304.2836](#))
- [36] Harrison B K, Thorne K S, Wakano M and Wheeler J A 1965 *Gravitation Theory and Gravitational Collapse* (Chicago: University of Chicago Press)
- [37] Misner C W, Thorne K S and Wheeler J A 1973 *Gravitation* (San Francisco: W.H. Freeman and Co.)
- [38] Shapiro S and Teukolsky S 1983 *Black holes, white dwarfs, and neutron stars: The physics of compact objects* (Wiley)
- [39] Friedman J L and Stergioulas N 2013 *Rotating Relativistic Stars* (Cambridge: Cambridge University Press)
- [40] Horbatsch M and Burgess C 2011 *JCAP* **1108** 027 (*Preprint* [1006.4411](#))
- [41] Pani P, Berti E, Cardoso V and Read J 2011 *Phys.Rev.* **D84** 104035 (*Preprint* [1109.0928](#))
- [42] Damour T and Esposito-Farèse G 1996 *Phys.Rev.* **D54** 1474–1491 (*Preprint* [gr-qc/9602056](#))
- [43] Harada T 1998 *Phys.Rev.* **D57** 4802–4811 (*Preprint* [gr-qc/9801049](#))
- [44] Freire P C, Wex N, Esposito-Farèse G, Verbiest J P, Bailes M *et al.* 2012 *Mon. Not. Roy. Astron. Soc.* **423** 3328 (*Preprint* [1205.1450](#))
- [45] Wex N 2014 (*Preprint* [1402.5594](#))
- [46] Doneva D D and Yazadjiev S S 2012 *Phys.Rev.* **D85** 124023 (*Preprint* [1203.3963](#))
- [47] Akmal A, Pandharipande V and Ravenhall D 1998 *Phys.Rev.* **C58** 1804–1828 (*Preprint* [nucl-th/9804027](#))
- [48] Demorest P B, Pennucci T, Ransom S M, Roberts M S E and Hessels J W T 2010 *Nature* **467** 1081–1083 (*Preprint* [1010.5788](#))
- [49] Antoniadis J, Freire P C, Wex N, Tauris T M, Lynch R S *et al.* 2013 *Science* **340** 6131 (*Preprint* [1304.6875](#))
- [50] Glampedakis K, Kapadia S J and Kennefick D 2014 *Phys.Rev.* **D89** 024007 (*Preprint* [1312.1912](#))
- [51] Hartle J B 1967 *Astrophys.J.* **150** 1005–1029
- [52] Hartle J B and Thorne K S 1968 *Astrophys.J.* **153** 807
- [53] Pani P and Berti E 2014 *Phys.Rev.* **D90** 024025 (*Preprint* [1405.4547](#))
- [54] Staykov K V, Doneva D D, Yazadjiev S S and Kokkotas K D 2014 *J. Cosmology Astropart. Phys.* **10** 006 (*Preprint* [1407.2180](#))
- [55] Lyne A, Burgay M, Kramer M, Possenti A, Manchester R *et al.* 2004 *Science* **303** 1153–1157 (*Preprint* [astro-ph/0401086](#))
- [56] Lattimer J M and Schutz B F 2005 *Astrophys.J.* **629** 979–984 (*Preprint* [astro-ph/0411470](#))
- [57] Kramer M and Wex N 2009 *Class.Quant.Grav.* **26** 073001
- [58] Doneva D D, Yazadjiev S S, Stergioulas N and Kokkotas K D 2013 *Phys.Rev.* **D88** 084060 (*Preprint* [1309.0605](#))
- [59] Berti E, White F, Maniopoulou A and Bruni M 2005 *Mon.Not.Roy.Astron.Soc.* **358** 923–938 (*Preprint* [gr-qc/0405146](#))
- [60] Kokkotas K and Ruoff J 2001 *Astron.Astrophys.* **366** 565 (*Preprint* [gr-qc/0011093](#))

- [61] Douchin F and Haensel P 2001 *Astron.Astrophys.* **380** 151 (*Preprint* [astro-ph/0111092](#))
- [62] Arponen J 1972 *Nucl.Phys.* **A191** 257–282
- [63] Novak J 1998 *Phys.Rev.* **D58** 064019 (*Preprint* [gr-qc/9806022](#))
- [64] Pani P, Cardoso V, Berti E, Read J and Salgado M 2011 *Phys.Rev.* **D83** 081501 (*Preprint* [1012.1343](#))
- [65] Yagi K and Yunes N 2013 *Science* **341** 365–368 (*Preprint* [1302.4499](#))
- [66] Yagi K and Yunes N 2013 *Phys.Rev.* **D88** 023009 (*Preprint* [1303.1528](#))
- [67] Pappas G and Apostolatos T A 2014 *Phys.Rev.Lett.* **112** 121101 (*Preprint* [1311.5508](#))
- [68] Yagi K, Kyutoku K, Pappas G, Yunes N and Apostolatos T A 2014 *Phys.Rev.* **D89** 124013 (*Preprint* [1403.6243](#))
- [69] Doneva D D, Yazadjiev S S, Staykov K V and Kokkotas K D 2014 *Phys.Rev.* **D90** 104021 (*Preprint* [1408.1641](#))
- [70] Doneva D D, Yazadjiev S S, Stergioulas N, Kokkotas K D and Athanasiadis T M 2014 *Phys.Rev.* **D90** 044004 (*Preprint* [1405.6976](#))
- [71] Sotani H and Kokkotas K D 2004 *Phys.Rev.* **D70** 084026 (*Preprint* [gr-qc/0409066](#))
- [72] Sotani H and Kokkotas K D 2005 *Phys.Rev.* **D71** 124038 (*Preprint* [gr-qc/0506060](#))
- [73] Silva H O, Sotani H, Berti E and Horbatsch M 2014 *Phys.Rev.* **D90** 124044 (*Preprint* [1410.2511](#))
- [74] Will C M and Zaglauer H W 1989 *Astrophys.J.* **346** 366
- [75] Zaglauer H 1992 *Astrophys.J.* **393** 685–696
- [76] Alsing J, Berti E, Will C M and Zaglauer H 2012 *Phys.Rev.* **D85** 064041 (*Preprint* [1112.4903](#))
- [77] Hunter J D 2007 *Computing In Science & Engineering* **9** 90–95